Effect of Oxygen Depletion Along the Air Channel of a PEMFC on the Warburg Diffusion Impedance

J. Mainka, G. Maranzana, J. Dillet, S. Didierjean, O. Lottin

Effect of oxygen depletion along the air channel of a PEMFC on the Warburg diffusion impedance

J. Mainka, G. Maranzana, J. Dillet, S. Didierjean, O. Lottin

LEMTA, Nancy University - CNRS, 2 avenue de la Forêt de Haye BP160, 54504 Vandoeuvre les Nancy Cedex, France.

The usual expression of the finite Warburg element used for analysing electrochemical impedance spectroscopy (EIS) spectra is obtained assuming that the reaction occurs at the electrode/membrane interface and that the oxygen concentration at the gas channel/gas diffusion layer interface is constant. A simple improvement of this expression consists in taking into account the oxygen concentration depletion along the gas channel. This pseudo-2D approach should be more appropriate for the investigation of mass transfer limitations in fuel cell membrane-electrode assemblies (MEA). Starting from experimental data from the literature, numerical simulations show that conclusions about the mass transfer limiting layer and its main characteristics can be significantly modified, which can contribute to a better understanding of oxygen transport in fuel cells. The results also put forward the existence of a critical value of the air stoichiometry below which, close to the air channel exit, no oxygen can access to the active layer. However, the diffusion impedance model does not take account of time dependent current variation effects on the gas concentration, although experimental (12,13) proofs have been brought, that they influence significantly the shape and the size of the measured impedance spectra.

Introduction

Fuel cell development has made considerable progress in recent years, so that their incorporation in mobile and stationary power applications becomes a realistic aim for the near future. Among the different categories of fuel cells (depending on the fuel and on the type of electrolyte), proton exchange membrane fuel cells (PEMFC) are very promising, because of their moderate operating conditions (temperatures lower than 100°C, gas pressures from 1 to 3 atm (1)). Using hydrogen as a fuel, they do not emit any greenhouse gases.

PEMFC fed with air must be able to operate at high current densities with a satisfying efficiency and reasonable gas consumption. Under these conditions, the slow oxygen diffusion to the cathode reaction sites represents a significant impediment, which has a direct influence on the oxygen reduction reaction (ORR) kinetics. Various works highlighted the limiting role of the gas diffusion layer for oxygen diffusion (2,3) in the porous cathode of a PEMFC. In this paper, we investigate the possibilities offered by Electrochemical Impedance Spectroscopy (EIS) for the identification of the main parameters governing the transport of oxygen at the cathode, including the effective

diffusivity D_{eff} , the characteristic thickness δ, and the porosity ε of the diffusion (equivalent) medium.

The first one-dimensional steady-state diffusion model proposed by Springer et al. (4) made it possible to analyse fuel cell's performance dependence on water management. Since, many improvements have been brought to the theoretical models. Most of them focus on charge and mass transfer at the cathode (5-7). For instance, Eikerling and Kornyshev (6) developed a model describing potential and concentration gradients through the active layer in the direction perpendicular to the electrode surface. In parallel, EIS allows to investigate the different processes occurring in PEMFCs (8) and to analyse *in situ* fuel cell's behaviour (9, 10). One of the most common expressions of the diffusion impedance in fuel cell equivalent circuits is that of the finite Warburg element (11), which yields results in good agreement with the experimental data, at least qualitatively. However, it is based on simple assumptions: Fick's diffusion, surface reaction, and a constant oxygen concentration at the interface with the gas channel. One way to improve the usual Warburg approach was proposed by Doyle et al. and Guo et al., who built pseudo-2D models for diffusion of lithium in batteries (31, 32) in order to estimate the diffusion coefficient D_s of lithium ions in the solid phase of the electrode. In the present work, we propose to improve the expression of the Warburg diffusion impedance by considering a decreasing oxygen concentration profile along the gas channel as an alternative boundary condition. This does not change radically the expression of the diffusion impedance, but has a significant impact on the size and on the shape of the impedance spectra, and as a result, on the identified values of the parameters characterising the transport of oxygen.

Note that oxygen depletion can be considered in terms of DC effects and in terms of AC effects. This work focuses on variations of the time-averaged oxygen concentration along the channel only; it does not describe the effects of oxygen concentration AC variations. The importance of these effects was recently pointed out by Schneider et al. (12,13) who showed experimentally that the AC signal applied for impedance measurement was at the origin of the oxygen concentration oscillations along the air channel, with a significant impact on the shape and size of the spectra. AC effects are more important at low frequency and at low air stoichiometry. They should also be linked to some geometrical parameters accounting for the capacity of the channel to store oxygen (its depth for instance) and they can appear even when the mass transfer resistance in the gas diffusion layer is negligible. Accounting for the oxygen concentration time-variation in the air channel would involve a full reconsideration of the diffusion impedance and to our knowledge, there is no analytical expression corresponding to this case in the literature. Therefore, the objective of this work is to put forward the limits of the 1D approach starting from the consideration of the decrease in the oxygen time-averaged concentration along the air channel.

Theoretical Model

Before accessing the active reaction sites, air and hydrogen have to flow through different media: the bipolar plates ensuring the gas supply via the flow-field channels, the gas diffusion layers (GDL) homogenising the gas propagation over the electrodes, and the catalyst layers consisting of a porous mixture of carbon powder and catalyst particles embedded in the electrolyte. Gases have to flow through the pores and the electrochemical reactions occur on (or in) the solid phase. Mass transfer models should take into account as well as possible the geometrical characteristics of these successive

media but actually, the finite Warburg element describes only gas diffusion through a homogeneous medium.

Model development

According to the majority of the authors (5,6,14), the oxygen reduction reaction is the main factor limiting the electrical efficiency of PEMFCs, even in optimal conditions. On top of that, the access of oxygen to the reaction sites remains problematic, due to the (possible) presence of liquid water in the MEA and to the low oxygen partial pressure when the fuel cell is fed with air (1). On the other hand, since the cathode is the place of water production, the ionic resistance of the well-hydrated polymer can be neglected. As a consequence, the main hypotheses of the one-dimensional cathode model, where oxygen transport occurs only by diffusion are:

- The fuel cell is assumed isothermal and isobaric.
- Ohmic drops in the active layers and in the GDLs are neglected.
- Mass transfer of O_2 and H_2O is assumed to occur only by diffusion in the pores of the active layer and of the GDL.
- Water diffusion through the solid phase of the active layer is not considered.

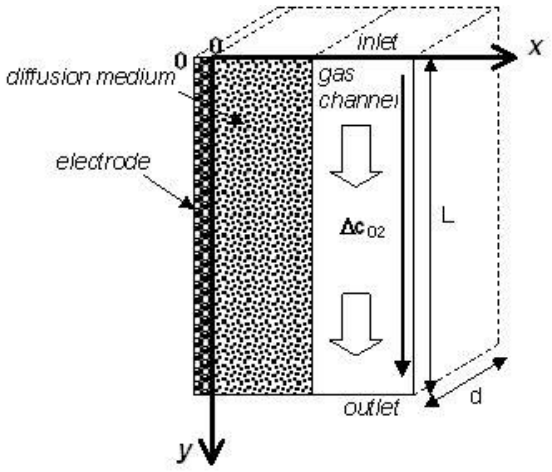

Figure 1. Schematic representation of the pseudo-2D diffusion model. Oxygen concentration depletion in the channel is taken into account for mass transfer modelling.

In order to obtain a pseudo-2D model (Figure 1) that takes into account the decrease in the oxygen concentration along the gas channel, three more hypotheses are made:

- The mass transfer resistance in the gas channel is neglected.
- Time variations of the oxygen concentration in the channel are neglected.
- The Tafel slope *b* is assumed to be constant between the inlet and the outlet of the air channel.

The gases flow along the channel length *L*; the electrode surface is given by $L \times d$. With these assumptions, the model can be considered as pseudo-two dimensional, the first dimension being the direction of oxygen diffusion from the channel to the active layer

whereas the second dimension is the direction of the channel, with a decrease in the time-averaged oxygen concentration.

Usually a Butler-Volmer formalism is used to describe oxygen reduction kinetics (15) but for sufficiently high current densities and in steady state, the activation overpotential follows a Tafel law of the form:

$$\eta_{act} = b \ln \frac{j_f(y) c_{02}^0}{j_0 c_{02}(x=0,y)} \qquad [1]$$

In equation [1], the faradaic current density $j_f\ (y)$ and the oxygen concentration $c_{O2}\ (x,y)$ vary along the gas channel, i.e. as functions of the *y* coordinate (Figure 1). The cell-averaged current density *J* is given by:

$$J = \frac{I}{Ld} = \frac{1}{L}\int_0^L j_f(y)\,dy \qquad [2]$$

By convention, the activation overpotential and the faradaic current density at the cathode side are usually negative. For convenience, we consider their absolute values: $j_f(y), \eta_{act} > 0$.

In the following, φ_{O_2} and φ_{H_2O} denote the fluxes in the *y* direction (in the air channel, in *Mol/s*) while N_{H_2O} and N_{O_2} denote the flux densities in the *x* direction (in the gas diffusion layer, in *Mol/s/m²*). The molar fluxes of oxygen φ_{O_2} and water φ_{H_2O} in the channel depend also on their *y*-position: $\varphi_{O2}(y)$ is equal to the molar fluxes of oxygen at the gas channel inlet $\varphi_{O_2}^{in}$ minus the amount consumed along the cathode:

$$\varphi_{O2}(y) = \varphi_{02}^{in} - \frac{d\int_0^y j_f(y)\,dy}{4F} \qquad [3]$$

As mentioned above, mass transfer along the *x* direction is assumed to occur only by diffusion, which means that the global molar flux density in the *x* direction $N_{H_2O} + N_{O_2}$ has to be null (Figure 1). This is a particular case that happens only when half of the water produced at the cathode is evacuated toward the air channel ($N_{H_2O} = j_f(y)/4F$) to compensate for the oxygen flux N_{O_2} in the opposite direction. The other half of the water produced by the cell, as well as the molecules flowing from the anode to the cathode under the effect of the electro-osmotic drag must diffuse through the membrane under the effect of a concentration gradient. Hence, the water flux along the gas channel φ_{H_2O} (in the *y* direction) is a function of *y*, given by:

$$\varphi_{H20}(y) = \varphi_{H20}^{in} + \frac{d\int_0^y j_f(y)dy}{4F} \quad [4]$$

Note that the question of the validity of the Warburg diffusion impedance in PEM fuel cells does not seem to have been fully addressed yet, considering that these operating conditions are not common: the net water drag coefficient can differ significantly from 0.5 (16). The fuel cell being fed by air, the oxygen molar ratio along the GDL/gas channel interface is given by:

$$y_{02}(y) = \frac{\varphi_{02}(y)}{\varphi_{02}(y) + \varphi_{N2} + \varphi_{H20}(y)} = \frac{\varphi_{02}^{in} - \frac{d\int_0^y j_f(y)dy}{4F}}{\varphi_{02}^{in} - \frac{d\int_0^y j_f(y)dy}{4F} + \varphi_{N2} + \varphi_{H20}^{in} + \frac{d\int_0^y j_f(y)dy}{4F}}$$

And since $\varphi_{N2} = 4\varphi_{O2}^{in}$, the above equation simplifies into:

$$y_{O2}(y) = \frac{S_{02} - \frac{d\int_0^y j_f(y)dy}{I}}{5S_{02}(1+H)}. \quad [5]$$

Where $S_{02} = \frac{\varphi_{02}^{in}}{I/4F}$ stands for the oxygen stoichiometry and $H = \frac{\varphi_{H20}^{in}}{\varphi_{02}^{in} + \varphi_{N2}}$ stands for the absolute humidity at the air inlet. Assuming that air is an ideal gas and that the mean oxygen concentration at the GDL/channel interface in AC conditions $\langle c_{02}(x=\delta, y)\rangle_t$ is equal to its steady-state value, it comes:

$$c_{02}(x=\delta, y) = \frac{P}{RT} y_{O2}(y) = \frac{P}{RT} \frac{S_{02} - \frac{d\int_0^y j_f dy}{I}}{5S_{02}(1+H)}. \quad [6]$$

The inlet concentration of oxygen in dry air being $c_{O2}^{0} = \frac{P}{5RT}$, the concentration along the air-channel/GDL interface $\left(x = \delta\right)$ can finally be expressed by:

$$c_{02}\left(x=\delta, y\right) = \frac{S_{02} - \frac{d\int_{0}^{y} j_f dy}{I}}{S_{02}\left(1+H\right)} c_{02}^{0}. \qquad [7]$$

According to the previous hypotheses, mass transport of oxygen through the pores of the diffusion media in a PEMFC is described by Stefan-Maxwell equations (1,17,18). However, since the binary diffusion coefficients of O_2/H_2O and O_2/N_2 are close to each other, it seems reasonable to use Fick's 1st law. Assuming that the electrochemical reaction takes place only at the active layer/membrane interface (x = 0), the 1st Fick's law can be written:

$$N_{O2}\left(y\right) = -D_{eff} \left.\frac{\partial c_{O2}}{\partial x}\right|_{\substack{x=0 \\ y}}. \qquad [8]$$

The diffusion media being porous, it is necessary to use an effective diffusion coefficient D_{eff} (19,20) taking into account their porosity ε and possibly, the presence of Knudsen diffusion (1,20). The most common expressions obey Archie's law (21,22):

$$D_{eff} = D\varepsilon^{m} \qquad [9]$$

Where m is an exponent varying between 1.5 and 4. In the case of a 3D medium, there is a wide consensus for using m = 3/2, which corresponds to the differential effective medium approximation introduced by Bruggeman (22,23). m = 3/2 is probably appropriate for active layers, in which the orientation of the solid phase does not follow a privileged direction (although this is not true in the agglomerate models using a cylindrical description (17,20)). In the gas diffusion layers however, the solid phase can be considered as two-dimensional since the carbon fibres are mainly parallel to the electrodes. In this case, the result of the differential effective medium theory is m = 2 (22). In a liquid, the diffusion is governed by shocks between the particles and D corresponds to the molecular diffusion coefficient D_{mol}. In a gas, two cases have to be distinguished depending on the values of the pore size and of the molecule's mean free path λ (17):

$$\lambda = \frac{RT}{\pi\sqrt{2}PN_A\sigma^2} \qquad [10]$$

Where N_A is the Avogadro number and σ the mean molecule diameter. If the mean free path is much smaller than the pore size ($\lambda << d_{pore}$) inter-molecular collisions govern the diffusion process and $D = D_{mol}$. If the mean free path is of the same range as the pore size ($\lambda \approx d_{pore}$), molecule collisions with the pore wall become significant and the Knudsen diffusion must be considered. This is not the case in the GDL where the typical

pore size is between 20 and 50 μm (24). On the other hand, Kong et al. (25) showed that in most of the active layers, the pore size is between 30 and 60 nm. Therefore, the Knudsen diffusion has to be taken into account. There exist various more or less sophisticated expressions combining D^K and D_{mol} for estimating the diffusion coefficient D. One of the most simple is the *Bosanquet formula* $\frac{1}{D} = \frac{1}{D_{mol}} + \frac{1}{D^K}$.

The Knudsen diffusion coefficient of species i can be expressed by $D_i^K = \frac{1}{3} d_{pore} \sqrt{\frac{8RT}{\pi M_i}}$.

DC solution

As the different species are neither consumed nor produced in the diffusion layers, their molar fluxes depend only on the y position. Nitrogen being inert, its flux density is null while the oxygen and water flux densities can be expressed as functions of $j_f(y)$:

$$N_{N2}(y) = 0, \qquad N_{O2}(y) = -\frac{j_f(y)}{4F}, \qquad N_{H_2O} = \frac{j_f(y)}{2F} + N_{H_2O}^m \qquad [11]$$

$N_{H_2O}^m$ stands for the amount of water diffusing through the membrane to the anode; according to the hypotheses leading to equation [4], $N_{H_2O}^m = -\frac{j_f(y)}{4F}$. In steady-state, Fick's 2nd law is given by:

$$0 = D_{eff} \frac{\partial^2 c_{02}}{\partial x^2}. \qquad [12]$$

Assuming that the oxygen reduction reaction takes place at the electrode/membrane interface ($x = 0$), equation [11] can be used as a boundary condition for the oxygen diffusion:

$$D_{eff} \left.\frac{\partial c_{O2}}{\partial x}\right|_{\substack{x=0 \\ y}} = \frac{j_f(y)}{4F}. \qquad [13]$$

Knowing the oxygen concentration at the channel/diffusion layer interface $(x = \delta)$ [7] allows to solve the Fick's diffusion equations in steady-state [12, 13], which yields the expression of $c_{O2}(x,y)$:

$$c_{02}(x,y) = \frac{IS_{02} - d\int_0^y j_f(y)\,dy}{IS_{02}(1+H)} c_{02}^0 - \frac{j_f(y)\delta}{4FD_{eff}}\left(1 - \frac{x}{\delta}\right). \qquad [14]$$

For comparison, the oxygen concentration in the classical 1D model is expressed by:

$$c_{02}(x) = c_{02}^{0} - \frac{J\delta}{4FD_{eff}}\left(1 - \frac{x}{\delta}\right) . \qquad [15]$$

The difference between [14] and [15] lies mainly in the oxygen concentration at the gas channel boundary. In the one-dimensional model, it is constant over the electrode surface, whereas in the two-dimensional model it varies between the gas inlet and the outlet. The pseudo-2D model takes also account of the air stoichiometry S_{O2} and of the gas humidification via the absolute humidity H at the fuel cell inlet.

AC solution

When a small sinusoidal perturbation $\Delta j_f\,(y,t)$ is added to the mean (DC) current density $\langle j_f(y)\rangle_t$, the oxygen concentration $c_{O2}(x,y,t)$ fluctuates around its steady-state value $\langle c_{02}(x,y)\rangle_t$ with the same frequency. The expressions of the current density and of the concentration must obey the following conditions:

$$\Delta c_{02}(x,y,t) = c_{02}(x,y,t) - \langle c_{02}(x,y)\rangle_t = \Delta\bar{c}_{02}(x,y)\exp(iwt) \qquad [16]$$

$$\Delta j_f(y,t) = j_f(y,t) - \langle j_f(y)\rangle_t = \Delta\bar{j}_f(y)\exp(iwt). \qquad [17]$$

The time-averaged value of the oxygen concentration $\langle c_{O2}(x,y)\rangle_t$ corresponds to the steady-state solution [14]:

$$\langle c_{02}(x,y)\rangle_t = \frac{IS_{02} - d\int_0^y \langle j_f(y)\rangle_t\, dy}{IS_{02}(1+H)} c_{02}^{0} - \frac{\langle j_f(y)\rangle_t\,\delta}{4FD_{eff}}\left(1 - \frac{x}{\delta}\right). \qquad [18]$$

Thus, in the expressions of the boundary conditions [7] and [13], the current density is replaced by its time-averaged value $\langle j_f(y)\rangle_t$. Fick's 2nd law in AC conditions is given by:

$$\frac{\partial c_{02}}{\partial t} = D_{eff}\frac{\partial^2 c_{02}}{\partial x^2} \qquad [19]$$

Replacing the oxygen concentration in the 2nd Fick's law by [16], it comes:

$$\Delta\bar{c}_{02}(x,y) = A(y)\cosh\left(\sqrt{\frac{jw}{D_{eff}}}x\right) + B(y)\sinh\left(\sqrt{\frac{jw}{D_{eff}}}x\right) \qquad [20]$$

Equation [13] yields the boundary condition at the electrode/membrane interface ($x = 0$), which makes it possible to determine $B(y)$:

$$D_{eff}\sqrt{\frac{jw}{D_{eff}}}\left(A(y)\sinh(0)+B(y)\cosh(0)\right)=\frac{\Delta\overline{j_f}(y)}{4F}$$

$$\Rightarrow B(y)=\frac{\Delta\overline{j_f}(y)}{4F\sqrt{jwD_{eff}}} \qquad [21]$$

Assuming that the signal variations are confined in the diffusion layers implicates that $\Delta c_{O2}(x=\delta,y,t)=0$, which yields for $A(y)$:

$$A(y)=-\frac{\Delta\overline{j}_f(y)}{4F\sqrt{jwD_{eff}}}\tanh\left(\sqrt{\frac{jw\delta^2}{D_{eff}}}\right) \qquad [22]$$

Then, $c_{O2}(x,y,t)$ is finally given by:

$$c_{02}(x,y,t)=\mathrm{Re}\left(-\frac{\Delta\overline{j}_f(y)}{4F\sqrt{jwD_{eff}}}\frac{\sinh\left(\sqrt{\frac{jw(\delta-x)^2}{D_{eff}}}\right)}{\cosh\left(\sqrt{\frac{jw\delta^2}{D_{eff}}}\right)}e^{iwt}\right)+\left\langle c_{O2}(x,y)\right\rangle_t \qquad [23]$$

At $x = 0$, the oxygen concentration variation $\Delta c_{02}(x=0,y,t)$ is given by:

$$\Delta c_{02}(x=0,y,t)=-\frac{\Delta\overline{j}_f(y)}{4F\sqrt{jwD_{eff}}}\tanh\left(\sqrt{\frac{jw\delta^2}{D_{eff}}}\right)\cdot e^{iwt}, \qquad [24]$$

Which makes it possible to express the faradaic impedance, defined as:

$$Z_f=\frac{\Delta\overline{\eta}_{act}}{\Delta\overline{j}_f}=\frac{\partial\eta_{act}}{\partial j_f}-\frac{\partial\eta_{act}}{\partial j_f}\frac{\partial j_f}{\partial c_{O2}}\frac{\Delta\overline{c}_{O2}}{\Delta\overline{j}_f}\bigg|_{x=0}. \qquad [25]$$

The first term $\frac{\partial\eta_{act}}{\partial j_f}$ in [25] is the charge transfer resistance R_{ct}:

$$R_{ct}(y)=\frac{b}{\left\langle j_f(y)\right\rangle_t}, \text{ in } \Omega\mathrm{cm}^2. \qquad [26]$$

The second term in [25] $-\frac{\partial\eta_{act}}{\partial j_f}\frac{\partial j_f}{\partial c_{O2}}\frac{\Delta\overline{c}_{O2}}{\Delta\overline{j}_f}\bigg|_{x=0}$ is the oxygen mass transfer impedance Z_{co2}. Its expression is obtained from [24] and [17]:

$$Z_{cO2}^{2D}(y) = b\frac{\tanh\left(\sqrt{\frac{jw\delta^2}{D_{eff}}}\right)}{4F\left\langle c_{02}(x=0,y)\right\rangle_t\sqrt{iwD_{eff}}}. \quad [27]$$

The oxygen concentration at $x = 0$ can be obtained with [18], so that the expression of the diffusion impedance [27] can also be written:

$$Z_{cO2}^{2D}(y) = R_d^{2D}\frac{\tanh\left(\sqrt{iw\tau_d}\right)}{\sqrt{iw\tau_d}}, \quad [28]$$

With the low frequency limit R_d^{2D}:

$$R_d^{2D} = \frac{b\delta}{4FD_{eff}\left\langle c_{02}(x=0,y)\right\rangle_t} \text{ , in } \Omega\text{cm}^2 \quad [29]$$

And the characteristic diffusion time τ_d:

$$\tau_d = \frac{\delta^2}{D_{eff}}. \quad [30]$$

The expression of the pseudo-2D diffusion impedance is close to that of the one-dimensional finite Warburg element (11):

$$Z_W = R_d^{1D}\frac{\tanh\left(\sqrt{iw\tau_d}\right)}{\sqrt{iw\tau_d}}, \quad [31]$$

With

$$R_d^{1D} = \frac{b\delta}{4FD_{eff}\left\langle c_{02}(x=0)\right\rangle_t}. \quad [32]$$

The characteristic diffusion time τ_d [30] is common to both cases.

Actually, the difference lies in the expression of the low frequency limit $R_d^{1D/2D}$: in the pseudo 2D model [29] the oxygen concentration $\left\langle c_{02}(x=0,y)\right\rangle_t$ depends on the y position and on the absolute humidity *H*, which should improve the precision of parameter estimation starting from the global diffusion impedance as well as from its local values along the cell surface.

Comparison of the 1D and pseudo-2D approaches

The pseudo-2D approach gives access to the global and local mass transfer characteristics under specified working conditions. In the following, data from the literature (18, 26) are analysed in order to open a discussion about its pertinence and interest.

Local mass transfer

The results that are discussed below come from data published by *Bultel et al.* (18) for a H_2/air PEMFC operating at 60°C with an inlet relative humidity RH of about 90%. The main parameters are summarized in Table I.

Table I: Values of the parameters used for the analysis of mass transfer (18).

T_{cell} [°C]	60
RH [-]	0.9
H [-]	0.2
P [atm]	1
S_{O2}[1] [-]	2 (if not mentioned otherwise)
A [cm^2]	0.5
L[1] [cm]	1
d[1] [cm]	0.5
δ_{GDL} [µm]	500 (if not mentioned otherwise)
ε_{GDL}	0.2
$D_{eff_{O2,H2O}}^{GDL}$ [$m^2\ s^{-1}$]	3.98 10^{-5} x ε_{GDL}^2
b [V dec^{-1}]	0.22
I [A]	0.25

An explicit expression of the diffusion resistance $R_d^{2D}(y)$ can be easily obtained from [29] and [18]:

$$R_d^{2D}(y) = \frac{b\delta}{4FD_{eff}\dfrac{IS_{O2} - d\int_0^y \langle j_f(y)\rangle_t\, dy}{IS_{O2}(1+H)}\, c_{O2}^0 - \langle j_f(y)\rangle_t\, \delta}. \qquad [33]$$

Figure 2 depicts profiles of $R_d^{2D}(y)$ corresponding to a constant current density $\langle j_f(y)\rangle_t = I/dL$. Large variations in the mass transfer resistance along the electrode surface can be observed. Furthermore, the profiles of $R_d^{2D}(y)$ are highly dependent on the air stoichiometry S_{O2}.

1 Hypothetical values added to complete the analysis

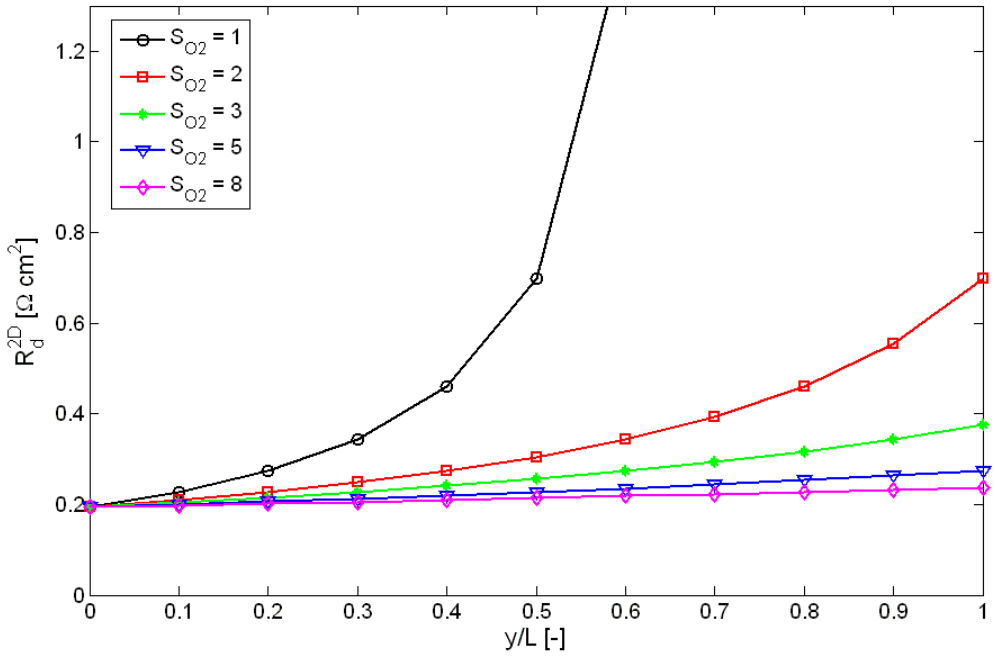

Figure 2. Profiles of $R_d^{2D}(y)$ between the air inlet and the air outlet for air stoichiometries varying from 1 to 8. The curves tend toward infinity for $S_{O2} < 1.44$ according to [34] and considering the values of the parameters given in Table I.

There is a critical value of the air stoichiometry $S_{O2}^{crit}(\delta)$ -function of the diffusion thickness δ- below which the oxygen concentration at the electrode/membrane interface $c_{O2}(x=0, y=L)$ becomes null near the gas channel outlet. As a consequence, R_d^{2D} tends toward infinity for S_{O_2} approaching $S_{O2}^{crit}(\delta)$. The expression of $S_{O2}^{crit}(\delta)$ is easily deduced from [14]:

$$S_{O2}^{crit} = \frac{c_{02}^0}{c_{02}^0 - \frac{J\delta}{4FD_{eff}}(1+H)} \qquad [34]$$

In the example of Figure 2, the value of $S_{O2}^{crit}(\delta)$ is about 1.44 and for $S_{O2} = 1$, there is no oxygen reaching the electrode/membrane interface beyond $y_{lim}/L = 0.69$. The analysis of the $R_d^{2D}(y)$ profiles makes it possible to determine in which conditions the diffusion impedance can be described by a one-dimensional model (when, for instance, the maximum relative variation over the electrode length $\Delta R_d^{2D}(L) = \left| \frac{R_d^{2D}(L) - R_d^{2D}(0)}{R_d^{2D}(0)} \right|$ is below 10%). In the conditions of table I (18), a one-dimensional behaviour would be achieved only for air stoichiometries S_{O2} above 11.

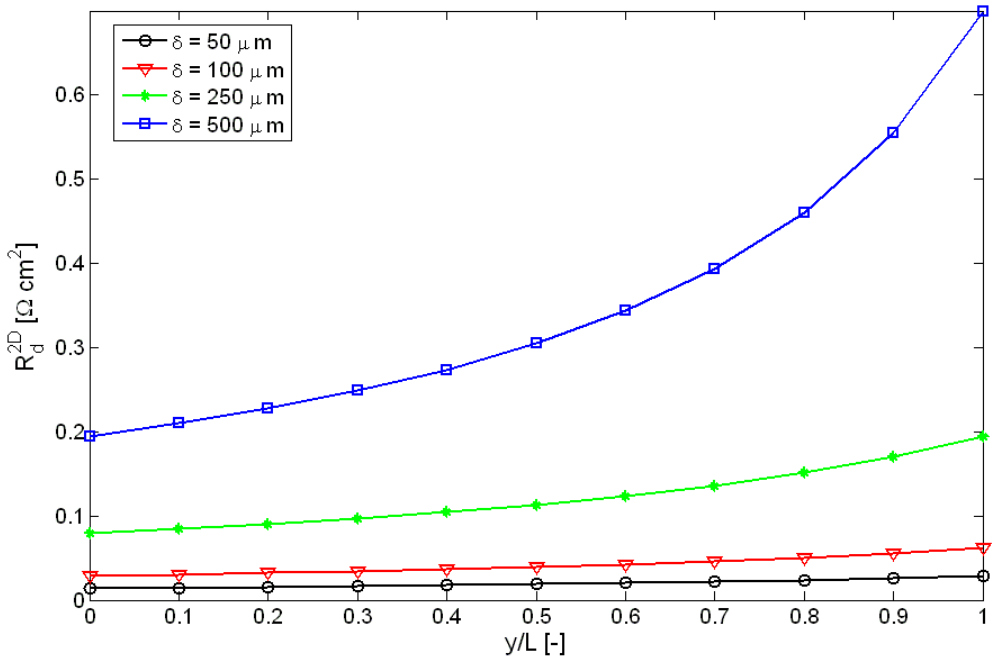

Figure 3. Profiles of $R_d^{2D}(y)$ between the air inlet and the air outlet for different values of the diffusion layer thickness and for a fixed air stoichiometry S_{O2} = 2 (starting from data of *Bultel et al.* (18), Table I).

The curves in Figure 3 confirm that the thickness of the diffusion layer has a significant impact on mass transfer kinetics. When S_{O2} = 2, reducing its initial value (500 µm (18)) by one half decreases significantly the mass transfer limitations: $\Delta R_d^{2D}(L)$ is reduced by a factor of 1.7. When S_{O2} = 4, $\Delta R_d^{2D}(L)$ is still reduced by a factor of 1.3 when dividing the diffusion layer thickness by one half.

Another way to estimate the effect of oxygen depletion is to compare the impedance spectra obtained with a usual finite Warburg element [31-32] and those obtained with the expression of the diffusion impedance derived above [28-29]. The results in Figure 5 correspond to the operating conditions of table I with an air stoichiometry S_{O2} = 3. The value of the characteristic diffusion time - τ_d = 0.751 *s* - is taken from an experimental work of *Rubio et al.* (26), performed in similar conditions. The frequency range is 1 *mHz* to 10 *kHz*.

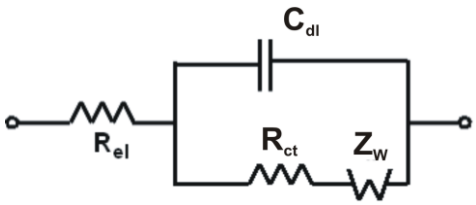

Figure 4. MEA equivalent electrical circuit according to Randles (30).

Figure 5 shows the impedance spectra of a whole fuel cell modelled using a Randles (30) equivalent circuit (Figure 4). This equivalent circuit consists of a membrane Resistance R_m, a charge transfer resistance R_{ct}, a double-layer capacity C_{dl} and a diffusion impedance Z_W (a finite Warburg element [31] or the diffusion impedance accounting for oxygen depletion along the air channel [28-29, 33]). The values of the impedances in the equivalent circuit -except the diffusion resistance- are taken from the experimental data of *Rubio et al*. (26). They are kept constant along the air channel, as well as the characteristic diffusion time τ_d, in order to put forward the effects of variations in the value of $R_d^{2D}(y)$ on the diffusion impedance: $R_{el} = 2.6\,\mathrm{m\Omega}$, $R_{ct} = 10.6\,\mathrm{m\Omega}$, $C_{dl} = 0.25\,F$ and $\tau_d = 0.751\mathrm{s}$ for a 100 cm^2 area single cell. As expected, the impedance spectra do not depend on the mass transfer impedance at frequencies above 10 Hz (5). In the low frequency range however (< 10 Hz), the higher values of the mass transfer resistance $R_d^{2D}(y)$ close to the air channel outlet impact significantly the shape and the size of the spectra. Note that the size of the low frequency loop corresponding to the finite Warburg impedance with $c_{O2}^0 = 0.21$ (i.e. with dry air) is significantly smaller than that obtained with the local value $Z_{cO2}(y/L = 0)$ accounting for the air humidity ($c_{O2}^0/(1+H) = 0.175$ - table I).

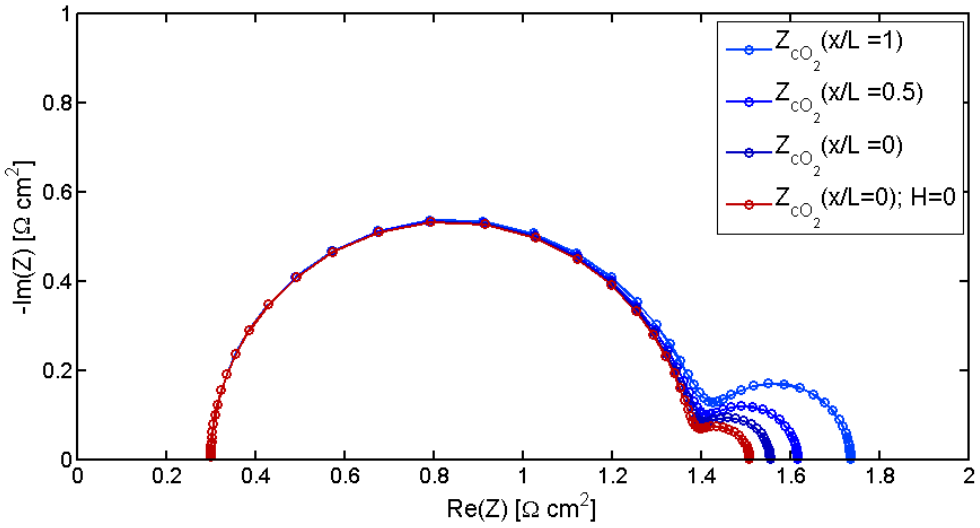

Figure 5. Comparison between a PEMFC impedance spectra obtained using a classical finite Warburg element [31] and spectra obtained using the diffusion impedance accounting for oxygen depletion [28-29/33]. The PEMFC is modelled using the Randles equivalent circuit (Figure 4). All the electrical parameters, except the diffusion impedance, are taken from experimental data measured by *Rubio et al*. (26).

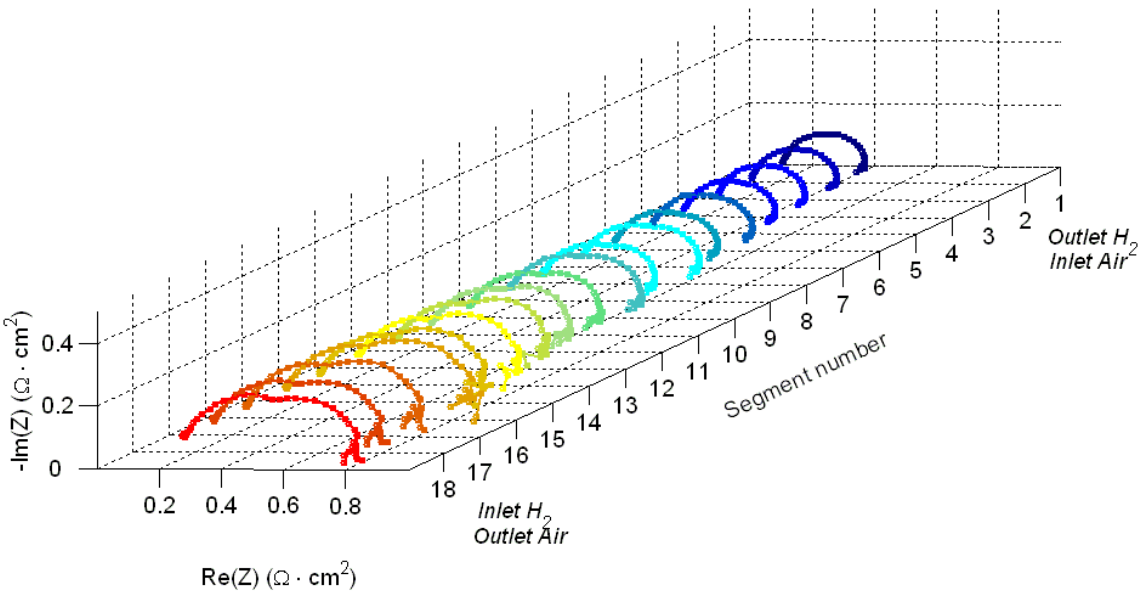

a)

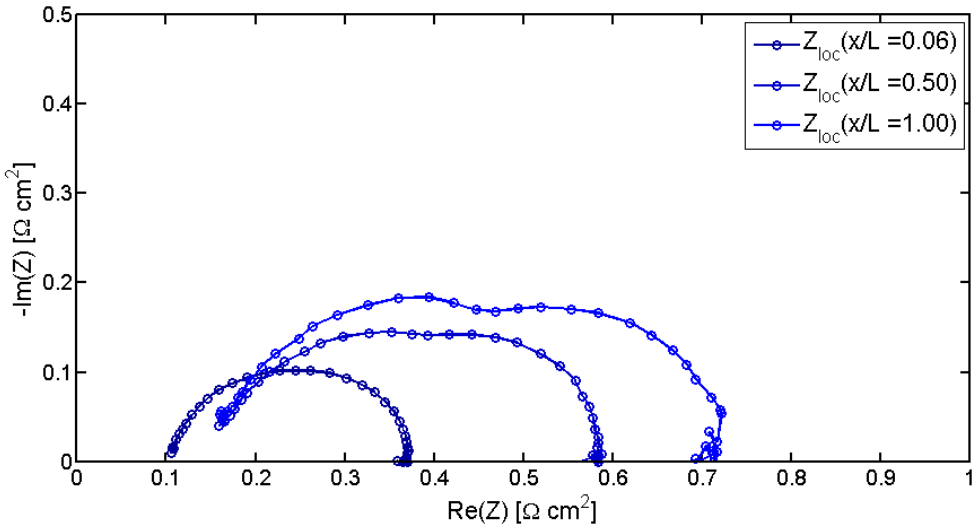

b)

Figure 6. Experimental impedance spectra measured along the cathode of a segmented PEMFC fed with pure hydrogen (S_{H2} = 1.2) and humidified air (S_{air} = 3) in counter-flow with a mean current density $\langle J \rangle_t = 0.5\,\mathrm{Acm^{-2}}$ (34). a) 3-D plot of the local impedance spectra. b) 2-D plot of the local experimental impedance spectra of segments 1 (x/L=0.06), 9 (x/L = 0.5) and 18 (x/L=1). The results show clearly the progressive appearance and enlargement of the low frequency loop along the air channel.

The numerical results of Figure 5 are confirmed by the shape of experimental spectra measured along the air channel of a segmented PEMFC (Figure 6). The fuel cell was fed

in counter flow with pure hydrogen (S_{H2} = 1.2) and humidified air (S_{air} = 3) and operated at a mean current density $\langle J \rangle_t = 0.5\,\mathrm{Acm^{-2}}$ (34). The experimental data on Figure 6a) show clearly the progressive enlargement of the low frequency loop along the air channel, from the inlet to the outlet. Note that in Figure 6a) and 6b), the low frequency loop cannot be distinguished in the impedance spectra of the firsts segments, probably because of the relatively large high frequency impedance at these locations whereas the (low frequency) mass transfer impedance is the lowest. Starting from expressions [28-29], the identification of the local mass transfer parameters (34) yields values that are in the typical range of PEMFC's gas diffusion layers. However, the results also show that for quantitatively reliable results, AC effects like those recently put forward by Schneider et al. (12, 13) have to be included in the oxygen transport model. Note that in the same way, the possible accumulation of liquid water near the air channel outlet (which should affect also the characteristic diffusion time τ_d) is not considered here.

Finally, some authors (33) mention the existence of a low frequency inductive loop that can be attributed to Pt oxidation. However, this phenomenon arises usually for frequencies of about 100 µHz or less, which is much lower than the frequency domain investigated in this work.

The simple modifications of the hypotheses leading to the expression of the Warburg impedance show that in usual conditions, mass transfer limitations due to oxygen consumption along the channel can be quite significant: the usual 1D approach remains satisfying only for large values of the air stoichiometry which do not correspond to usual operating conditions.

Mass transport properties of the diffusion medium

EIS can be used to estimate the mass transport properties of the diffusion layers. Since $R_d^{1D/2D}$ and τ_d depend on the diffusion medium thickness δ, on the effective diffusivity D_{eff}, and indirectly on the porosity ε [9], these parameters can be identified by fitting experimental impedance spectra. Starting from the expression of the characteristic diffusion time τ_d [30], of $R_d^{1D/2D}$ [32, 33] and of the charge transfer resistance R_{ct} [26], one can obtain relations that allow to determine the thickness of the limiting diffusion medium δ [35, 36]. These expressions depend on the operating conditions and on the impedance parameters τ_d and $R_d^{1D/2D}$, which must be identified experimentally:

$$\delta^{1D} = \frac{\tau_d J}{4F c_{02}^0}\left(\frac{R_{ct}}{R_d^{1D}} + 1\right). \qquad [35]$$

$$\delta^{2D}(y) = \frac{\langle j_f(y)\rangle_t \tau_d}{\dfrac{IS_{02} - d\int_0^y \langle j_f(y)\rangle_t \, dy}{IS_{02}(1+H)}}\left(\frac{R_{ct}}{R_d^{2D}} + 1\right). \qquad [36]$$

Actually, equation [36] expresses δ as a function of y. A global estimation of the diffusion thickness can be obtained by using the mean value of equation [36] over the

electrode length L. In the absence of other information, assuming a homogeneous current density, $\left\langle j_f \right\rangle_t (y) = J$, it comes:

$$\left\langle \delta^{2D} \right\rangle_L = \frac{J\tau_d}{4F c_{02}^0 \dfrac{S_{02} - \dfrac{1}{2}}{S_{02}(1+H)}} \left(\frac{R_{ct}}{R_d^{2D}} + 1 \right). \qquad [37]$$

Then, the effective diffusivity D_{eff} and the porosity ε corresponding to this value of δ can be determined with [30] and [9], respectively. δ and ε can be compared to the actual thickness and porosity of the gas diffusion layer and of the active layer, which provides indications about the main origin of oxygen transport limitation. Furthermore, comparing the results of equations [35] and [36] tells whether oxygen transport can be considered as one dimensional or two-dimensional. Examples of results are presented in the following, starting from another set of data measured by *Rubio et al.* (26) with a single PEM cell of 100 cm^2 operated at $I = 12.5\ A$ at 1 *atm*. The fuel cell was fed by pure H_2 and dry air with a stoichiometry S_{O2} = 2.3 (26). In these conditions, the charge transfer resistance was R_{ct} = 13.2 mΩ and the diffusion resistance was R_d = 7.97 mΩ. Since the cell temperature was not given, it has to be estimated, as well as the air inlet relative humidity. Knowing that the fuel cell was not humidified, we chose T_{cell} = 60 °C and H = 0.1, which is equivalent to a mean RH equal to *0.5* in the channel. The identified values for δ and D_{eff} are given in Table II.

Table II: Diffusion thickness δ and effective diffusion coefficient identified starting from experimental results of *Rubio et al.* (26) and comparison with typical values from the literature (29,30). Oxygen is assumed to diffuse in gas phase through the GDL and the active layer: the possible presence of liquid is accounted for via the actual value of the porosity ε.

Model	**δ [m]**	**D_{eff} [$m^2\ s^{-1}$]**	**ε_{GDL}**	**ε_{AL}**
1D	$0.834\ 10^{-3}$	$9.94\ 10^{-7}$	0.18	0.27
pseudo 2D	$1.2\ 10^{-3}$	$1.99\ 10^{-6}$	0.25	0.43
Literature	GDL: $0.42\ 10^{-3}$ (29) AL: $10\ 10^{-6}$ (est.)	GDL: $3.2\ 10^{-5} \times \varepsilon_{GDL}^2$ AL: $6.9\ 10^{-6} \times \varepsilon_{AL}^{3/2}$ (27)	0.2 - 0.6 (5)	0.2 – 0.35 (28)

The differences between the parameters identified using the usual Warburg expression and the one resulting from the pseudo-2D approach show clearly that gas consumption along the air channel has an influence, at least in these operating conditions. The values of the diffusion thickness δ and of the effective diffusion coefficient D_{eff} estimated using the pseudo-2D diffusion impedance are higher: the difference ranges from about 30% for the porosity ε to about 100% for the effective diffusion coefficient. The classical one-dimensional Warburg expression yields a value of the effective diffusion coefficient $D_{eff} = 9.94 10^{-7}\ m^2 s^{-1}$, which is typical for active layers [$6.2\ 10^{-7}$ $m^2 s^{-1}$ – $1.4\ 10^{-6}$ $m^2 s^{-1}$; Table II]; the corresponding value of the porosity (starting from an equivalent -molecular and Knudsen- diffusion coefficient equal to $6.9\ 10^{-6} \times \varepsilon_{AL}^{3/2}$ [9]) is also within the range generally considered for active layers. However, the estimated diffusion thickness is almost 2 orders of magnitude higher than the typical thickness of an active layer (≈ 10 μm). Hence, a clear conclusion about the limiting layer for mass transfer is not possible with the 1D approach. Using the pseudo-2D approach [37], both the porosity and the equivalent diffusion coefficient are within ranges typical of gas

diffusion layers. The estimated thickness $\delta_{2D} = 1.2\ 10^{-3}$ m is about 3 times larger than the actual GDL thickness ($\delta = 0.42\ 10^{-3}$ m (29)), but this could be the result of gas diffusion in the *y* direction below the channel rib (which would increase the total diffusion thickness) and/or by a possible mass transfer resistance in the gas channel: the gas diffusion layer seems to be the limiting medium for oxygen diffusion, which is in agreement with some previous works (18).

Conclusions and perspectives

EIS is frequently used to investigate the origin of the mass transfer impedance in cathode gas diffusion and active layers. However, the expression of a finite Warburg element used for analysing impedance spectra is obtained assuming that the oxygen concentration at the gas channel/gas diffusion layer interface is constant: this hypothesis is not valid for usual values of the air stoichiometry, and it can lead to wrong estimates of the mass transfer parameters characterising the diffusion media. An alternative approach is proposed: considering gas consumption along the gas channel entails minor changes to the classical Warburg expression and numerical simulations starting from experimental data from the literature show that conclusions about the mass transfer limiting layer and its main characteristics can be significantly modified. The estimated thickness of the GDL is significantly higher than the actual value, which could be linked to a possible mass transfer resistance in the gas channel and/or to constriction effects below the channel rib.

These first results are mostly of qualitative interest and should be confirmed shortly by specific experiments. On top of that, it should be noted that there still exists a wide range of possible improvements in the analytical expression of the diffusion impedance, among which:

- The consideration of oxygen concentration time-variation in the air channel (12, 13).
- The consideration of all possible values of the water flux, always assumed equal to $N_{H_2O} = j_f(y)/4F$ in the present models.
- The consideration of the 3D structure of the electrode, and of the distribution of the oxygen consumption through the electrode.

These issues will be the purpose of future works, which should allow a more accurate estimation of the main mass transfer parameters and of the limiting diffusion layer as functions of the operating conditions and of the position along the air channel.

References

1. J. Deseure, *J. Power Sources*, **178**, 323 (2008).
2. E. Passalacqua, G. Squadrito, F. Lufrano, A. Patti and L. Giorgi, *J. Appl. Electrochem.*, **31**, 449 (2001).
3. J. Ihonen, M. Mikkola and G. Lindbergh, *J. Electrochem. Soc.*, **151**, 1152 (2004).
4. T.E. Springer, T.A. Zawodzinski and S. Gottesfeld, *J. Electrochem. Soc.*, **138**, 2334 (1991).
5. T.E. Springer, T.A. Zawodzinski, M.S. Wilson and S. Gottesfeld, *J. Electrochem. Soc.*, **143**, 587 (1996).
6. M. Eikerling and A.A. Kornyshev, *J. Electroanal. Chem.*, **475**, 107 (1999).
7. Y. Bultel, L. Genies, O. Antoine, P. Ozil and R. Durand, *J. Electroanal. Chem.*, **527**, 143 (2002).
8. J.R. Selman and Y.P. Lin, *Electrochim. Acta*, **38**, 2063 (1993).
9. N. Wagner, *J. Appl. Electrochem.*, **32**, 859 (2002).
10. B. Andreaus, A.J. McEvoy and G.G. Scherer, *Electrochim. Acta*, **47**, 2223 (2002).
11. E. Warburg, *Ann. Phys. Chem.*, **67**, 493 (1899).
12. I.A. Schneider, S.A. Freunberger, D. Kramer, A. Wokaun and G.G. Scherer, *J. Electrochem. Soc.*, **154(4)**, B383-B388 (2007).
13. I.A. Schneider, D. Kramer, A. Wokaun and G.G. Scherer, *J. Electrochem. Soc.*, **154(8)**, B770-B782 (2007).
14. J. Kim, S.-M. Lee, S. Srinivasan and C.E. Chamberlin, *J. Electrochem. Soc.*, **142**, 2670 (1995).
15. S. Srinivasan and H.D. Hurwitz, *Electrochim. Acta*, **12**, 495 (1967).
16. T. Colinart, S. Didierjean, A. Chenu, O. Lottin, S. Besse, Experimental study on water transport coefficient in Proton Exchange Membrane Fuel Cell, *J. Power Sources*, **190(2)**, 230 (2009).
17. J. Ramousse, J. Deseure, O. Lottin, S.Didierjean and D. Maillet, *J. Power Sources*, **145**, 416 (2005).
18. Y. Bultel, K. Wiezel, F. Jaouen, P. Ozil and G. Lindbergh, *Electrochim. Acta*, **51**, 474 (2005).
19. D. Armost and P. Schneider, *Chem. Eng. J.*, **57**, 91 (1995).
20. M. Boillot, Phd dissertation, INPL-ENSIC, Nancy (2005).
21. G. E. Archie, Trans. AIME **146**, 54-61 (1942).
22. S. Torquato, *Random Heterogeneous Materials: Microstructure and Macroscopic Properties*, Springer (2002).
23. H. C. Bruggeman, Berechnung verschiedener Physikalischer Konstanten von heterogenen Substanzen, *Ann. Physik (Leipzig)* **24,** 636-679 (1935).
24. P. Argyropoulos, K. Scott, W. M. Taama, *J. Appl. Electrochem*. **29,** 661-669 (1999).
25. C. S. Kong, D. Y. Kim, H. K. Lee, Y. G. Shul, T. H. Lee, *J. Pow. Sources* **108,** 185-191 (2002).
26. M.A. Rubio, A.Urquia, R.Kuhn and S.Dormido, *J. Power Sources*, **183**, 118 (2008).
27. R. B. Bird, W. E. Stewart and E. N. Lightfoot, *Transport Phenomena*, p.517, John Wiley and Sons, Inc. (2002).
28. A. Fischer, J. Jindra and H. Wendt, *J. Appl. Electrochem.*, **28**, 277 (1998).
29. Sigracet®, *www.servovision.com/fuel_cell_components/gdl_10.pdf*.
30. J.E.B. Randles, *Discuss. Faraday Soc.*, **1**, 11 (1947).

31. Q. Guo, V.R. Subramanian, J.W. Weidner, R.E. White, *J. Electrochem. Soc.*, **149(3)**, A307-A318 (2002).
32. M. Doyle, J.P. Meyers, J. Newman, *J. Electrochem. Soc.*, **147(1)**, 99-110 (2000).
33. M. Mathias, D. Baker, J. Zhang, Y. Liu, W. Gu, *ECS Transactions*, **13(13)**, 129-152 (2008).
34. J. Mainka, G. Maranzana, J. Dillet, S. Didierjean, O. Lottin, *Proceedings* **WHEC 18**/ 16-21 May 2010, Essen Germany (2010).

Nomenclature

A	Electrode area (m^2)
b	Tafel slope ($V\ dec^{-1}$)
c_{O2}	Oxygen concentration ($mol\ m^{-3}$)
c_{O2}^{0}	Oxygen inlet concentration in dry air ($mol\ m^{-3}$)
d	Electrode width (m)
D	Diffusion coefficient ($m^2\ s^{-1}$)
D_{eff}	Effective diffusion coefficient ($m^2\ s^{-1}$)
D_i^K	Knudsen diffusion coefficient ($m^2\ s^{-1}$)
D_{mol}	Molecular diffusion coefficient ($m^2\ s^{-1}$)
F	Faraday's constant ($C\ mol^{-1}$)
H	Absolute humidity (-)
I	Cell current intensity (A)
j_f	Faradic current density ($A\ cm^{-2}$)
j_0	Exchange current density ($A\ cm^{-2}$)
J	Cell current density ($A\ cm^{-2}$)
L	Gas channel length (m)
M_i	Molar weight ($kg\ mol^{-1}$)
N_A	Avogadro number (mol^{-1})
N_i	Molar flux ($mol\ m^{-2}\ s^{-1}$)
P	Pressure (Pa)
R	Universal gas constant ($J\ mol^{-1}\ K^{-1}$)
RH	Relative Humidity (-)
R_{tc}	Charge transfer resistance ($\Omega\ cm^2$)
$R_d^{1D/2D}$	Low frequency limit of the diffusion resistance (Ω)
S_{O2}	Oxygen stoichiometric ratio (-)
T	Temperature (K)
y_{O2}	Oxygen molar ratio (-)
Z_{cO2}^{2D}	pseudo-2D diffusion impedance ($\Omega\ cm^2$)
Z_f	Faradaic impedance ($\Omega\ cm^2$)
Z_W	finite Warburg ($\Omega\ cm^2$)

Greek letters

δ	Layer thickness (m)
ε	Porosity (-)
η_{act}	Activation overpotential (V)
λ	Mean free path (m)
φ_i	Molar flux ($mol\ s^{-1}$)
σ	Mean particle diameter (m)
τ_d	Characteristic diffusion time (s)
ω	Angular frequency (s^{-1})

Subscripts

AL	Active layers
GDL	Gas diffusion layer
H_2O	Water
N_2	Nitrogen

O_2 Oxygen